

Please cite this article in press as: Shenton FC, Pyner S. Expression of transient receptor potential channels TRPC1 and TRPV4 in venoatrial endocardium of the rat heart. *Neuroscience* (2014), <http://dx.doi.org/10.1016/j.neuroscience.2014.02.047>

Neuroscience xxx (2014) xxx–xxx

EXPRESSION OF TRANSIENT RECEPTOR POTENTIAL CHANNELS TRPC1 AND TRPV4 IN VENOATRIAL ENDOCARDIUM OF THE RAT HEART

F. C. SHENTON AND S. PYNER*

School of Biological & Biomedical Sciences, Durham University, Durham DH1 3LE, UK

Abstract—The atrial volume receptor reflex arc serves to regulate plasma volume. Atrial volume receptors located in the endocardium of the atrial wall undergo mechanical deformation as blood is returned to the atria of the heart. The mechanosensitive channel(s) responsible for regulating plasma volume remain to be determined. Here we report that the TRP channel family members TRPC1 and TRPV4 were expressed in sensory nerve endings in the atrial endocardium. Furthermore, TRPC1 and TRPV4 were coincident with the nerve ending vesicle marker synaptophysin. Calcitonin gene-related peptide was exclusively confined to the myo- and epicardium of the atria. The small conductance Ca^{2+} -activated K^+ channels (SK2 and SK4) were also present, however there was no relationship between SK and TRP channels. SK2 channels were expressed in nerves in the epicardium, while SK4 channels were in some regions of the endocardium but appeared to be present in epithelial cells rather than sensory endings. In conclusion, we have provided the first evidence for TRPC1 and TRPV4 channels as potential contributors to mechanosensation in the atrial volume receptors. © 2014 Published by Elsevier Ltd. on behalf of IBRO.

Key words: TRPC1, TRPV4, synaptophysin, atrial volume receptor, mechanosensation, SK channels.

INTRODUCTION

Cardiovascular fluid homeostasis is essential for survival. The atrial volume reflex arc is an important contributor to the maintenance of bodily homeostasis, primarily responding to blood volume changes (Hainsworth, 1991). This reflex is initiated by cardiac mechanoreceptors known as atrial volume or low pressure receptors located at the venous atrial junction of the heart. The receptors are activated as blood is returned to the atria. Mechanical deformation of the

atrial wall is transduced into a neural signal, which vagal afferent fibers (arising from the atrial volume receptors) conduct toward the nucleus tractus solitarius (Spyer, 1994). The information is integrated centrally, for example, in the paraventricular nucleus of the hypothalamus (Affleck et al., 2012) to bring about changes in the level of sympathetic activation that promotes water and electrolyte output from the kidney (Ledsome and Linden, 1964; Kappagodda et al., 1973). Paintal (1953) was probably the first to provide electrophysiological characteristics of the receptors. Information regarding their exact location and morphology is sparse and conflicting, although they are reported to be found mainly in the endocardial layer of the atrial wall (Woollard, 1926; Coleridge et al., 1957; Holmes, 1957; Tranumjensen, 1975; Thoren et al., 1979; Hainsworth, 1991; Cheng et al., 1997). Details of the molecular machinery underpinning the transduction mechanism so far remain unknown.

Recent advances in understanding the molecular mechanisms of mammalian mechanotransduction systems have led to the identification of possible candidates for mechanosensitive channel proteins (Delmas et al., 2011). These include the epithelial Na channel/degenerin/acid sensing ion channel (ENaC/DEG/ASIC) and the transient receptor potential (TRP) families. A role for the ENaC/DEG/ASIC family in mechanotransduction in rat muscle spindles has recently been described (Simon et al., 2010). The TRP family proteins have been implicated in mechanosensation in the heart (Inoue et al., 2009). Baroreceptor terminals innervating the aortic arch and carotid sinus in rats were found to express the γ subunit of ENaC (Drummond et al., 1998). In mice, ASIC1, 2 and 3 were found in aortic baroreceptor neurons in the nodose ganglia and their terminals in the aortic arch (Lu et al., 2009). Furthermore, ASIC2 null mice exhibit impaired baroreflex control and develop hypertension, thus providing evidence that compromised mechanosensing within the cardiovascular system could contribute to cardiovascular disease (Lu et al., 2009). The ASIC3 channel would appear to be important for blood volume control in mice (Lee et al., 2011) and be associated with calcitonin gene-related peptide (CGRP) in the nerve terminals in the venous atrial junction area.

Few studies have looked at TRP expression in mechanosensory organs and endings despite the fact they are considered to be strong candidates as mechanosensitive channels in mammals (Inoue et al.,

*Corresponding author. Tel: +44 (0)191 3341346.

E-mail address: susan.pyner@durham.ac.uk (S. Pyner).

Abbreviations: AF, Alexa Fluor; ANP, atrial natriuretic peptide; BSA, bovine serum albumin; CGRP, calcitonin gene-related peptide; ENaC/DEG/ASIC, epithelial Na channel/degenerin/acid sensing ion channel; FCS, fetal calf serum; IR, immunoreactivity; PBS, phosphate-buffered saline; SK, small conductance Ca^{2+} -activated K^+ channels; SYN, synaptophysin; TRP, transient receptor potential.

2009). A pressure-induced calcium influx that was gadolinium, but not lanthanide sensitive has been demonstrated in baroreceptor neurons from nodose ganglia of rats (Sullivan et al., 1997). These results suggest that stretch-activated channels, for which TRP channels are leading molecular candidates, could be the mechanotransducers in baroreceptors (Watanabe et al., 2008). TRPC1 and TRPC3–5 are present not only in the soma of nodose ganglion sensory neurons but also in the peripheral axons and mechanosensory endings that terminate as mechanosensitive receptors in the aortic arch of the rat (Glazebrook et al., 2005).

We used antibodies directed toward synaptophysin (SYN) or CGRP to identify sensory nerve terminals within the endocardium in the right atrial cardiac tissue and combined these with anti-channel antibodies, focusing on proteins of the ENaC/DEG/ASIC and TRP families as potential contributors to the mechanotransduction process. Afferent output from rat muscle spindle endings is subject to autogenic modulation by glutamate that is Ca^{2+} dependant (Bewick et al., 2005) and Ca^{2+} -activated K^+ channels have been shown to regulate the discharge frequency from these endings (Banks et al., 2009). Furthermore in rat atria the Ca^{2+} -activated K^+ channel isoform SK4 is involved in the release of atrial natriuretic peptide (ANP) in response to stretch (Ogawa et al., 2009). Therefore we also tested for the presence of Ca^{2+} -activated K^+ channels SK1–4 as potential modulators of atrial volume receptor excitability.

EXPERIMENTAL PROCEDURES

Ethics statement

Three male Hooded Lister rats were humanely killed in strict accordance with the Code of Practice for the Humane Killing of Animals under Schedule 1 of the Animals (Scientific Procedures) Act 1986. The protocol was approved by Durham University Life Sciences Ethical Review Panel.

Tissue preparation for immunohistochemistry

The atria, including entrances of the major vessels, were removed and fixed overnight in 4% formaldehyde at 4 °C. Following cryoprotection in sucrose/phosphate-buffered saline (PBS), venoatrial regions known to contain atrial volume receptors were dissected out, frozen and 16- μm cryosections collected onto poly-L-lysine coated slides. Sections were allowed to air dry for 1 h at room temperature, the slides were then stored briefly at -20 °C before use. On the day of the assay, slides were removed from the freezer and air dried again for one hour.

Immunohistochemistry

Sections were blocked for 45 min at room temperature in PBS pH 7.4 containing 0.4% Triton X-100, 4% fetal calf serum (FCS) and 1% bovine serum albumin (BSA). The antibody diluent for both the primary and secondary antibodies was PBS pH 7.4 containing 0.1% Triton X-100, 1% FCS and 1% BSA. After the blocking stage

sections were incubated for 48 h at 4 °C with a pair of primary antibodies (see Sections ‘Sensory neurons’, ‘Mechanosensitive channels’, and ‘Small conductance Ca^{2+} -activated K^+ channels (SK1–4)’ for details). Following this, the sections were rinsed and washed in PBS (3 \times 10 min), and then Alexa Fluor (AF) secondary antibodies applied for 1 h (either goat anti-rabbit-AF 594 and goat anti-mouse-AF 488, or donkey anti-goat-AF 594 and donkey anti-mouse-AF 488). See Table 1 for details and concentrations of primary and secondary antibodies. The slides were rinsed and washed in PBS as before and mounted in PBS/glycerol.

Sensory neurons. Rabbit anti-CGRP and mouse anti-SYN antibodies were used to identify sensory neurons. Secondary antibodies were goat anti-rabbit-AF 594 and goat anti-mouse-AF 488. All secondary antibodies were used as described above (Section ‘Immunohistochemistry’).

Mechanosensitive channels. Anti-channel antibodies (ASIC2, ASIC3, αENaC , βENaC , γENaC , TRPC1, TRPC4/5, TRPC6, TRPV4) were used together with mouse anti-SYN. These were all rabbit antibodies, with the exception antibodies to ASIC2, ASIC3 and TRPC6, which were raised in goat. Secondary antibodies were either goat anti-rabbit-AF 594 and goat anti-mouse-AF 488, or donkey anti-goat-AF 594 and donkey anti-mouse-AF 488; as appropriate. Rabbit anti-TRPV4 and mouse anti-CGRP (goat anti-rabbit-AF 594 and goat anti-mouse-AF 488 as secondaries) was also used.

Small conductance Ca^{2+} -activated K^+ channels (SK1–4). SK1 and SK3 antibodies were raised in goat, SK2 and SK4 in rabbit. They were used with mouse anti-SYN as the sensory neuron marker. Secondary antibodies were either donkey anti-goat-AF 594 and donkey anti-mouse-AF 488 or goat anti-rabbit-AF 488 and goat anti-mouse-AF 594, as appropriate.

Antibody specificity. These are all commercial antibodies subject to routine quality assurance (see Table 1 for details). Where positive results were obtained the pattern of reactivity was distinctive to that particular antibody with specific structures consistently labeled by that antibody on repeat assays. Furthermore anti-TRPV4 immunoreactivity (IR) was absent in tissue from TRPV4 $^{-/-}$ mice using this same commercial antibody (Girard et al., 2013). Similarly anti-TRPC1-specific staining in C2C12 myoblasts was significantly reduced following TRPC1 silencing with TRPC1-siRNA (Meacci et al., 2010). We have used the antibodies against ENaC/DEG/ASIC proteins (with the exception of anti-ASIC3) in a previous study investigating mechanotransduction in rat muscle spindles (Simon et al., 2010). We have used the SK 1–3 antibodies to examine the expression of SK channels in lanceolate endings of hair follicles in the rat (Shenton et al., 2010).

Specificity of the secondary antibodies was confirmed by incubating control sections in PBS with the omission of primary antibodies. With this regime no staining was observed.

Table 1. Details of primary and secondary antibodies

Primary antibodies							
Antibody	Host	Poly/monoclonal Purification method	Immunogen	Manufacturer	Catalog No.	Concentration or dilution	Manufacturer's quality control
<i>Sensory neurons</i>							
Anti-SYN	Mouse	Mono clone SY38 protein A purified	Vesicular fraction of bovine brain	Millipore	MAB5258	1 µg/ml	WB mouse brain lysates, single band 38 kDa
Anti-CGRP	Mouse	Mono clone 4901 protein G purified	Rat alpha-CGRP	Abcam	Ab81887	1/80	IHC DRG, pancreas and gut
Anti-CGRP	Rabbit	Polyclonal whole antiserum	Full length rat CGRP conjugated to bovine THY	Abcam	Ab43873	1/300	ICC rat amygdala and spinal cord
<i>Mechanosensitive channels</i>							
ASIC2 (E-20)	Goat	Polyclonal affinity purified	Epitope mapping at the N-terminus of human ASIC2	Santa Cruz	sc-22333	5 µg/ml	WB rat brain, band at 65 kDa
ASIC3	Goat	Polyclonal whole antiserum	Synthetic peptide from the extracellular domain of rat ASIC3	Abcam	Ab101595	1/280	WB recombinant peptide
αENaC (H-95)	Rabbit	Polyclonal proprietary method	aa 131-225 near the N-terminus of human αENaC	Santa Cruz	sc-21012	5 µg/ml	WB human recombinant αENaC fusion protein
βENaC (H-190)	Rabbit	Polyclonal proprietary method	aa 271-460 within an internal region of human βENaC	Santa Cruz	sc-21013	5 µg/ml	WB human βENaC transfected 293T cell lysates
γENaC (H-110)	Rabbit	Polyclonal proprietary method	aa 411-520 near the C-terminus of human γENaC	Santa Cruz	sc-21014	5 µg/ml	WB cell lysates: A549, Caki-1 and COLO 320DM cells
TRPC1 (H-105)	Rabbit	Polyclonal proprietary method	aa 689-793 mapping at the C-terminus of human TRPC1 origin	Santa Cruz	sc-20110	5 µg/ml	WB mouse and rat testis, band 83 kDa
TRPC4/5 (H-80)	Rabbit	Polyclonal proprietary method	aa 1-80 within an N-terminal cytoplasmic domain of human TRPC5	Santa Cruz	sc-28760	5 µg/ml	IF mouse heart
TRPC6 (C-13)	Goat	Polyclonal affinity purified	peptide mapping at the C-terminus of human TRPC6	Santa Cruz	sc-19197	5 µg/ml	IHC human rectum tissue
TRPV4	Rabbit	Polyclonal affinity purified	Synthetic peptide KLH conjugated, derived from within residues 850 to the C-terminus of mouse TRPV4	Abcam	Ab39260	5 µg/ml	WB vs mouse brain lysates
<i>Small conductance Ca²⁺-activated K⁺ channels</i>							
SK1 (A-13)	Goat	Polyclonal proprietary method	Epitope mapping near the C-terminus of human SK1	Santa Cruz	sc-17991	5 µg/ml	WB rat and mouse brain
SK2	Rabbit	Polyclonal affinity purified	aa 542-559 mapping within the intracellular C-terminus of rat SK2	Alomone	APC-028	2 µg/ml	WB rat brain membranes
SK3 (H-17)	Goat	Polyclonal proprietary method	Epitope mapping within an internal region of human SK3	Santa Cruz	sc-16027	5 µg/ml	WB PC-12 cell lysate
SK4	Rabbit	Polyclonal affinity purified	aa 350-363 mapping within the intracellular C-terminus of rat SK4	Alomone	APC-064	2 µg/ml	WB in rat and human tissue

Image acquisition, visualization and analysis

Sections were examined using a Zeiss Axioskop 2 under epifluorescence. Digital images were captured with a Hamamatsu Orca 285 CCD camera controlled by Improvion Volocity (Acquisition, Restoration and Visualisation) software (v. 6.2.1). Images were obtained and processed in a similar manner to that described previously (Affleck et al., 2012). For selected images a series of z-stacks were acquired. The 3D volume was deconvolved using iterative restoration and the appropriate Point Spread Function which models the spread of light in the optical path that causes blur. This process reassigned out-of-focus haze without subtracting it from the data to improve resolution in the X, Y and Z planes. This produced a confocal-like quality image. The most appropriate single Z plane image was then converted to a 3-D Opacity image, which is a high-resolution render with options to display data in different views. The isosurface view is a form of indirect rendering, which identifies a surface around objects where all voxel intensity values are the same. Isosurface rendering generates a 3D non-transparent solid of the surface elements. The max intensity view applies direct maximum intensity projection rendering. The brightest intensity in the view path to the screen will form the image. These image manipulations can improve clarity and thereby help in the visualization of sites where differentially labeled proteins may coincide and interact.

The final images were imported into Adobe Photoshop (CS4 extended v. 11.02), which was used to adjust brightness and contrast. Processed images were grouped into plates and labeled in Adobe Photoshop.

RESULTS

Sensory neurons

SYN labeling. SYN-IR was widely expressed in all three layers of the atrial wall. In the endocardium, where atrial volume receptors are expected to be predominantly located SYN-IR was dense and complex

in places (Fig. 1A) with an appearance characteristic of similar mechanosensory endings (Drummond et al., 1998; Maeda et al., 1999). In the myocardium SYN-IR was also present in the vicinity of structures with the appearance of small blood vessels (Fig. 1A). In the epicardium SYN-IR was found in nerves and around putative ganglion cells and blood vessels (not shown).

CGRP labeling. By contrast CGRP-IR was rarely seen in the endocardial layer (Fig. 1B). It was occasionally present in the myocardium, mostly in association with blood vessel-like structures (Fig. 1B) where there was overlap with SYN labeling (Fig. 1C); but also on some nerve endings within this layer (Fig. 3E). Immunoreactivity for CGRP was intense in the epicardium around putative ganglion cells and blood vessels, and within nerve fibers (not shown).

Mechanosensitive ion channels

TRPC1 labeling. Immunoreactivity for mechanosensitive ion channels revealed the presence of TRPC1 (Fig. 2). Immunoreactivity for this channel was coincident with SYN-IR in the endocardium (Fig. 2C, C') and myocardium (not shown), although SYN-IR was always more prevalent. The isosurface view (Fig. 2C') suggests that while the TRPC1 and SYN labeling are closely associated, they may be localized to different compartments within the sensory nerve terminals. Immunoreactivity for TRPC1 was not found around ganglion cells in the epicardium (not shown), even where SYN labeling was evident.

TRPV4 labeling. TRPV4 labeling was particularly widespread in both the endocardium (Fig. 3B, E) and myocardium (Fig. 3E). In these layers TRPV4-IR and SYN-IR always coincided (Fig. 3C, C'). TRPV4-IR was far more abundant than CGRP-IR in both endocardium and myocardium, especially in endocardium where CGRP was rarely expressed (Fig. 3D–F'). Although far less prevalent, CGRP labeling was present on some TRPV4-positive endings (Fig. 3F, F'). The isosurface

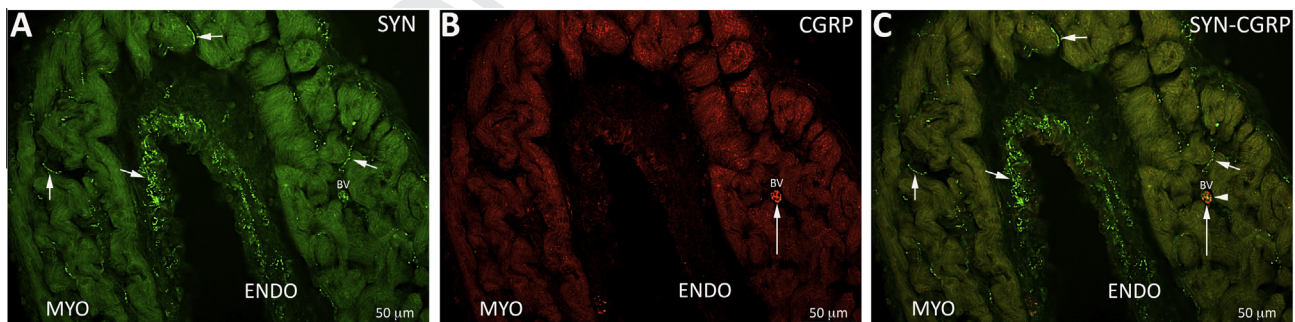


Fig. 1. Sensory neurons: synaptophysin and calcitonin gene-related peptide labeling. Double labeling with mouse anti-synaptophysin (green SYN A, C) and rabbit anti-calcitonin gene-related peptide (red CGRP B, C) antibodies. SYN-immunoreactivity (SYN-IR) (short arrows A, C) was present in all three layers of the cardiac wall. In the endocardium (ENDO) SYN-IR was dense and complex, compared to the myocardium (MYO) where it was sparse. SYN-IR was also evident in the location of blood vessel-like structures (BV). CGRP-IR was occasionally expressed in the myocardium, especially around blood vessels (long arrow B) where there was some overlap with SYN-IR (arrowhead C); but CGRP-IR did not appear to extend into endocardium. (For interpretation of the references to color in this figure legend, the reader is referred to the web version of this article.)

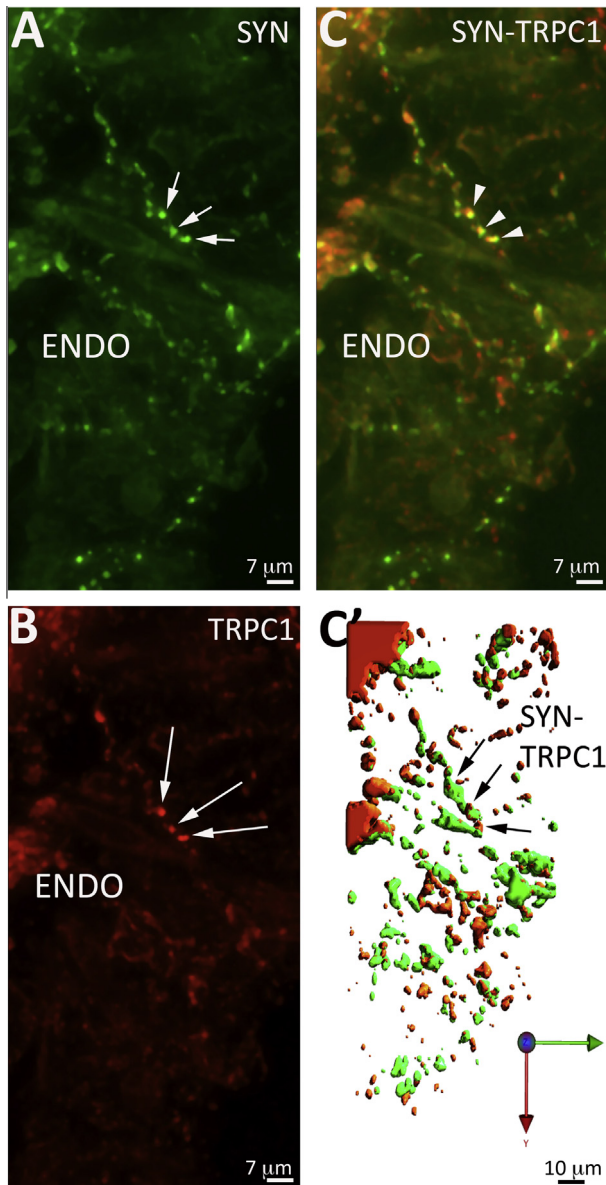


Fig. 2. Mechanosensitive ion channels: Transient Receptor Potential Canonical 1 (TRPC1) labeling in the endocardium. Double labeling with mouse anti-SYN (green SYN A, C, C') and rabbit anti-TRPC1 (red TRPC1 B, C, C') antibodies. SYN immunoreactivity (short arrows A) and TRPC1-IR (long arrows B) were both evident within the endocardium. Panel C is the merge of A and B, TRPC1-IR coincided with SYN-IR labeling on nerve endings (arrowheads C). Panel C' is a 3-D Opacity image displayed as an isosurface to demonstrate more clearly the concurrence and compartmentalization of TRPC1 and SYN labeling (black arrows C'). (For interpretation of the references to color in this figure legend, the reader is referred to the web version of this article.)

views were again suggestive of compartmentalization of TRPV4 labeling compared with either SYN (Fig. 3C') or CGRP (Fig. 3F') expression on the same ending. In contrast to TRPC1, TRPV4-IR was also evident around ganglion cells in the epicardium where it coincided with SYN-IR labeling (not shown).

There was a complete absence of immunoreactivity for ENaC/DEG/ASIC family members: α ENaC, β ENaC,

γ ENaC, ASIC2 or ASIC3. Also for the TRP family members, TRPV1 and TRPC4–6 again no immunoreactivity was evident.

Small conductance Ca^{2+} -activated K^+ channels

SK2 labeling. For small conductance Ca^{2+} -activated K^+ channel SK2 immunoreactivity (SK2-IR) was evident in nerve bundles within the epicardium, although it did not coincide with SYN-IR in this location (not shown). However, SK2-IR was only very occasionally present within the myocardium possibly extending into the endocardium (Fig. 4B) and here there was SK2-SYN co-labeling (Fig. 4C–C'), although the reactivity did not precisely overlap, suggestive of compartmentalization (Fig. 4C', C').

SK4 labeling. Small conductance Ca^{2+} -activated K^+ channel SK4 immunoreactivity (SK4-IR) was found in the endocardium giving small patches of diffuse labeling that appeared to be over epithelial cells (Fig. 4E). SK4-IR was clearly distinct from SYN-IR in this layer (Fig. 4F). There was an absence of SK1 or SK3 immunoreactivity throughout the heart tissue.

DISCUSSION

This study has provided the first evidence of the conductance channels present in putative atrial volume receptors within the endocardium of the right atria of the rat. The TRP family channels TRPC1 and TRPV4 were expressed, however there was no evidence to indicate the presence of ENaC/DEG/ASIC proteins. These findings suggest mechanotransduction in atrial volume receptors may rely on the TRP family of channels, which contrasts with the baroreceptor and muscle spindle where ENaC/DEG/ASIC channel families have been reported (Drummond et al., 1998; Simon et al., 2010) and are therefore candidates as the mechanotransducers in these endings.

Calcium-activated K^+ channel, SK2 and SK4 were occasionally present in both the endo- or myocardial layers. Based on the appearance of the putative AVR's identified by the sensory nerve terminal marker SYN (see Section 'Synaptophysin labeling'), we suggest SK2 and SK4 may not form part of the molecular components of an AVR.

SYN and CGRP as markers of sensory nerve terminals: putative atrial volume receptors

The vesicle marker SYN was abundantly expressed in all three layers of the cardiac wall. SYN is used to identify the synaptic vesicles in presynaptic endings. Furthermore synaptic-like vesicles have commonly been described in mechanosensory endings of vertebrate and invertebrate animals (Katz, 1966). The pattern of SYN-IR observed in the endocardium was characteristic of sensory endings (Drummond et al., 1998; Maeda et al., 1999) and therefore likely to be labeling atrial volume receptors. Previous histological studies describe atrial

267
268
269

270

271
272
273
274
275
276
277
278
279
280

281
282
283
284
285
286
287

288

289
290
291
292
293
294
295
296
297
298
299
300
301

302
303
304
305
306
307
308

309
310

311
312
313
314
315
316
317
318
319
320

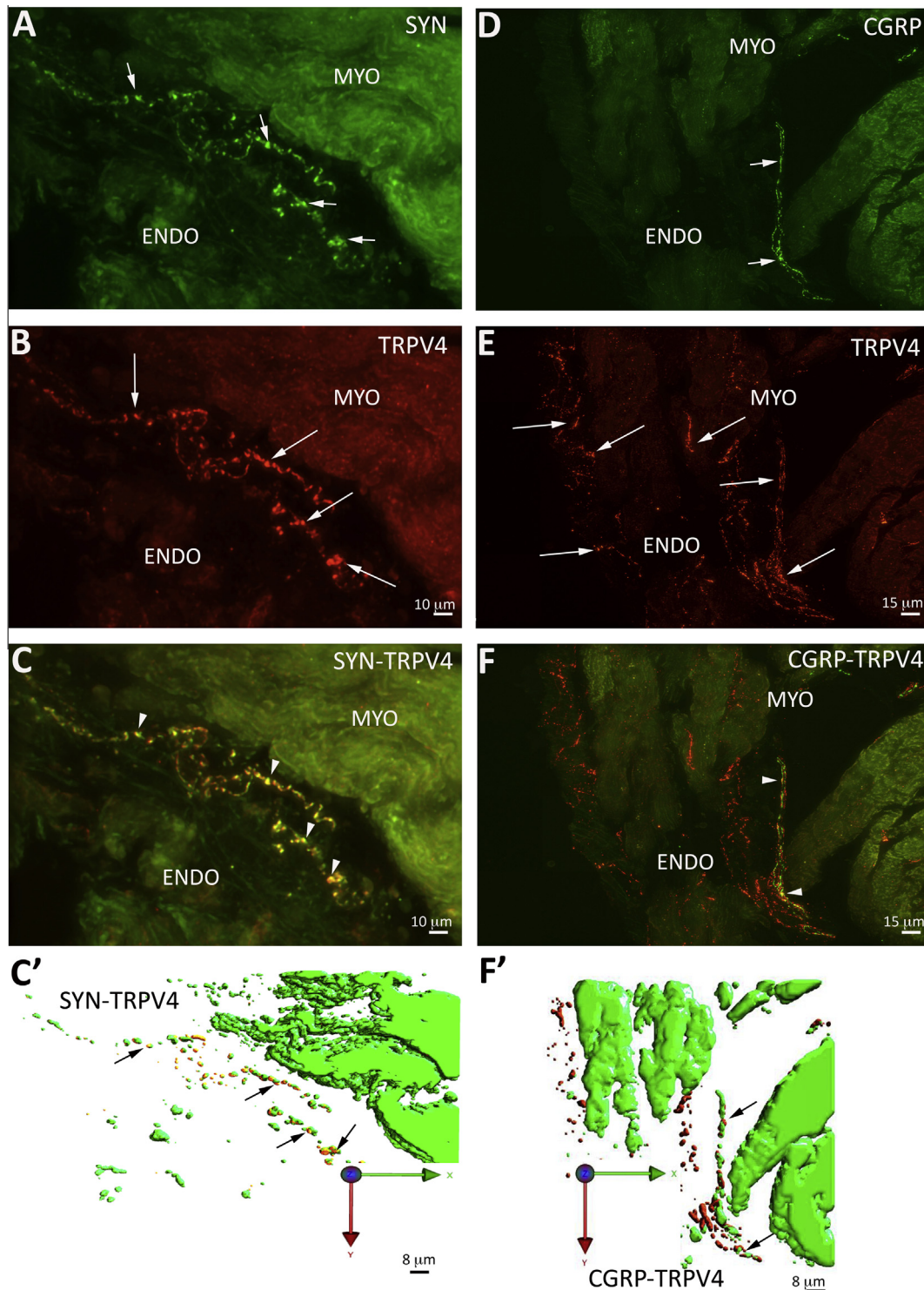


Fig. 3. Mechanosensitive ion channels: Transient Receptor Potential Vanilloid 4 (TRPV4) labeling in endocardium and myocardium. Double labeling with rabbit anti-TRPV4 (red TRPV4 B, C, C', E, F, F') and either mouse anti-SYN (green SYN A, C, C') or mouse anti-CGRP (green CGRP D, F, F') antibodies. TRPV4 immunoreactivity (TRPV4-IR) (long arrows B, E) was widespread in the endocardium (ENDO) and also extended into the myocardium (MYO). Nerve endings identified by SYN-IR (short arrows A) were colabeled with anti-TRPV4 antibodies (arrowheads C). Panel C' is the isosurface presentation of a Volocity 3D slice to illustrate the close relationship between TRPV4 and SYN labeling (black arrows C', indicate concurrent TRPV4–SYN labeling). CGRP-IR was only rarely found in either endocardium or myocardium (short arrows D). However, on the occasions when it was present the endings were also TRPV4 positive (arrowhead F). Panel F' is the isosurface presentation of a Volocity 3D slice to illustrate the presence of CGRP labeling on TRPV4-positive endings (black arrows F', indicate dual labeling). The isosurface views (C', F') are again indicative of anti-channel and sensory nerve labeling occurring in distinct compartments within the same ending. (For interpretation of the references to color in this figure legend, the reader is referred to the web version of this article.)

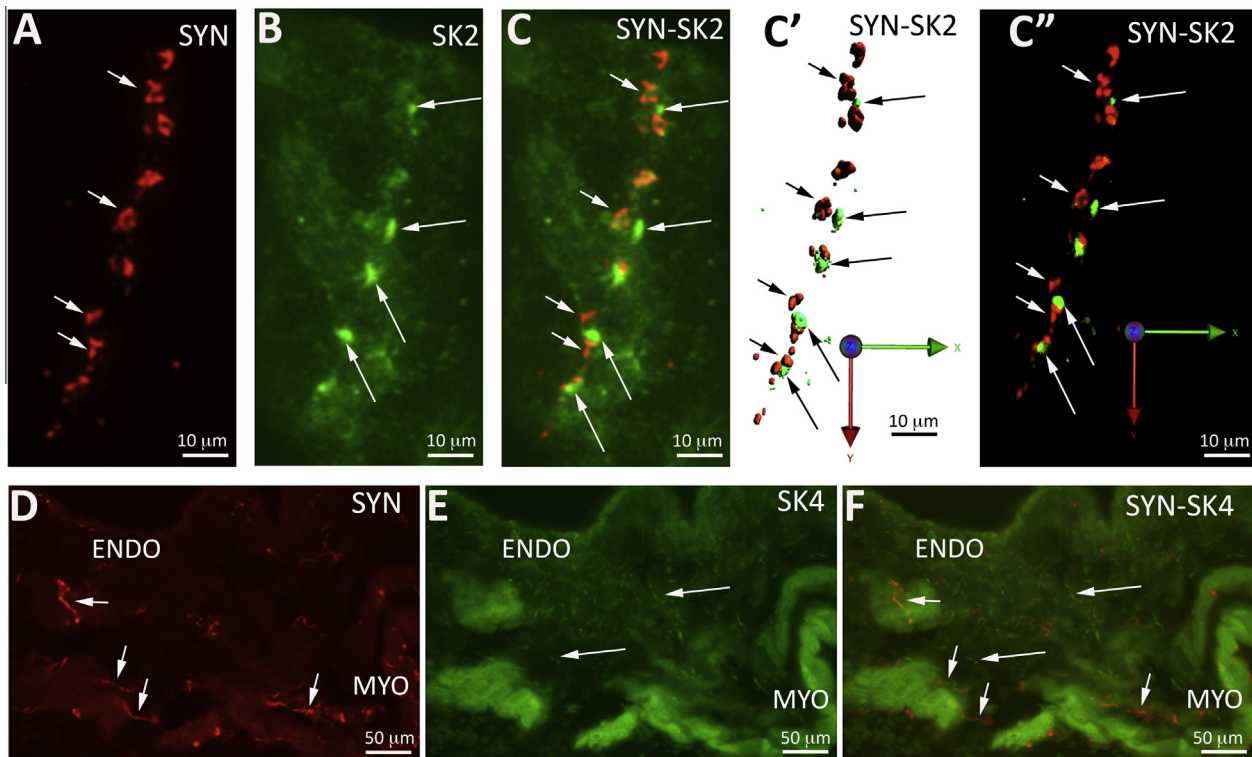


Fig. 4. Small conductance Ca^{2+} -activated K^+ channels SK2 and SK4 labeling in the endocardium. Double labeling with either rabbit anti-SK2 (green SK2 B, C, C', C'') or rabbit anti-SK4 (green SK4 E,F) antibodies and mouse anti-SYN (red SYN A, C, C', C'', D, F) antibodies. SK2 immunoreactivity (SK2-IR) (long arrows B, C) was occasionally identified within the myocardium and possibly extending into the endocardium and here the endings were both SK2 and SYN (short arrows A,C) positive. Panel C' and C'' are isosurface and max intensity presentations respectively, to give clearer views of the SK2–SYN dual labeling. Although the labeling appeared to be closely apposed in places (black arrows C') it did not precisely co-localise. SK4 immunoreactivity (SK4-IR) (long arrows E, F) occurred as occasional diffuse patches, which appeared to be over epithelial cells in the endocardium (ENDO). The SK4-SYN merge (F) clearly shows that SK4-IR (long arrows F) did not coincide with the SYN-IR (short arrows F) present in this layer. (For interpretation of the references to color in this figure legend, the reader is referred to the web version of this article.)

321 volume receptors as predominantly within the endocardial
 322 layer ideally placed to sense blood volume changes
 323 (Coleridge et al., 1957; Holmes, 1957; Tranumjensen,
 324 1975; Thoren et al., 1979; Cheng et al., 1997). Based
 325 on the detailed description of vagal afferents carried out
 326 by Cheng et al. (1997), the SYN-IR we observed around
 327 ganglion cells in the epicardium was probably efferent
 328 rather than afferent innervation. SYN-IR within the
 329 myocardium was slightly less dense than in the other
 330 two layers. Presumptive atrial volume receptors have
 331 also been shown to extend into myocardium
 332 (Tranumjensen, 1975) and it has been suggested that
 333 atrial volume receptors in these various locations could
 334 account for the different types based on
 335 electrophysiological classification (Kappagoda et al.,
 336 1976).

337 In our hands CGRP-IR was not as widespread as
 338 SYN-IR and it seldom extended into the endocardium.
 339 CGRP-IR was strongest in the epicardium surrounding
 340 ganglion cells, blood vessels and within nerve fibers.
 341 These findings are in agreement with a study in which
 342 only 9% of vagal afferent neurons, identified by injecting
 343 the retrograde tracer cholera toxin B-subunit into the
 344 pericardium, were found to be CGRP positive (Corbett
 345 et al., 2005). There was seldom co-localization of CGRP
 346 and SYN-IR in any of the tissue layers and this,

347 together with the distribution pattern, suggests that
 348 CGRP is not a marker for mechanosensory afferents
 349 here. CGRP- labeling of volume receptor nerve
 350 terminals in the venoatrial junction has been found co-
 351 localized with ASIC3-IR (Lee et al., 2011). However, it is
 352 not certain that the endings described here were in the
 353 endocardium.

354 CGRP- has been associated with the regulation of
 355 sympathetic activity (Oh-hashii et al., 2001). However,
 356 our observations suggest that in respect to blood
 357 volume at least, this is more likely to be mediated via
 358 CGRP-positive neurons located within the central
 359 nervous system where it is widely expressed in the
 360 medulla, a region involved in cardiovascular regulation
 361 (Skofitsch and Jacobowitz, 1985). We seldom found
 362 CGRP-IR in the endocardium, and conclude it did not
 363 appear to be present in atrial volume receptor afferents.

Mechanosensitive ion channels

364 Immunoreactivity for TRPC1 and TRPV4 was found
 365 within the atrial tissue and in particular the endocardial
 366 layer. Where TRPV4-IR was observed around ganglion
 367 cells in the epicardium, the innervation is most probably
 368 efferent (Cheng et al., 1997). Around ganglion cells in
 369 the epicardium TRPV4 reactivity was observed, but not
 370

TRPC1-IR. Again this innervation around ganglion cells is most probably efferent (Cheng et al., 1997). The TRPC1 and TRPV4-IR always coincided with SYN-IR, suggestive of labeling of putative atrial volume receptors where it was present within the endocardium. Since our CGRP-labeling experiments suggested this peptide was not expressed in atrial volume receptor afferents (see Section ‘Discussion’), only limited assays were undertaken using anti-mechanosensitive ion channel antibodies in combination with anti-CGRP antibodies.

Surprisingly, no immunoreactivity for ENaC (α ENaC, β ENaC, γ ENaC) or ASIC (ASIC2, ASIC3) was evident in any area of the atrial tissue examined. Amiloride sensitive channels play a role in mechanotransduction in rat muscle spindles (Simon et al., 2010) and these are likely to be ENaC/DEG/ASIC-related proteins. The antibodies used in this present study were the same as those used by ourselves in rat muscle spindles where we detected immunoreactivity to ENaC (α ENaC, β ENaC, γ ENaC), and ASIC2 in primary mechanosensory afferents (Simon et al., 2010). Therefore, our evidence would suggest that mechanotransduction in the atrial volume receptors is dependent upon a different set of channel proteins.

In muscle spindle terminals primarily a Na^+ current underpins mechanotransduction (Hunt et al., 1978). TRP channels are non-selective Ca^{2+} channels (Ramsey et al., 2006), therefore the ionic basis for the current in atrial volume receptors is likely to be different from that observed in spindle terminals. Interestingly, gadolinium, a non-selective blocker of stretch-activated ion channels, reduced blood volume expansion effects on urine flow, neural activation, and ANP release both in ASIC3 $^{-/-}$ and ASIC3 $^{+/+}$ control mice (Lee et al., 2011). Furthermore, gadolinium also blocks TRP channels including TRPV4 (Jung et al., 2003; Becker et al., 2005); suggesting that other molecular components, for example TRP channels, in addition to ASIC3 can contribute to blood volume control.

The ASIC2 channel located in the nodose ganglia and aortic arch has been shown to be an important component of the arterial baroreceptor reflex in mice (Lu et al., 2009). A pressure-induced calcium influx has been demonstrated in baroreceptor neurons from the nodose ganglia of rats with characteristics compatible with TRP channels (Sullivan et al., 1997). The TRPC1 channel appears to be important for cardiovascular regulation, affecting vascular tone and smooth muscle depolarization in response to pressure load (Inoue et al., 2009). Our finding of TRPC1 immunoreactivity in putative mechanosensory endings in the right atrium, suggests that TRPC1 activation in this location could in addition initiate or regulate the atrial volume receptor reflex arc.

It is probable that TRPV channels function as part of multiprotein complexes (Suzuki et al., 2005; Fu et al., 2006; Huai et al., 2012), where different components of the complex may regulate TRPV expression and underlie tissue-specific sensing modalities (D’Hoedt et al., 2008). For example, in mice, within the parvocellular neurons of the paraventricular nucleus,

TRPV4 and SK channels are involved in osmosensing (Feetham and Barrett-Jolley, 2012). Interestingly, it has recently been demonstrated that TRPV4 forms heteromeric channels with TRPC1 in vascular endothelial cells (Ma et al., 2010) and this TRPV4-C1 complex mediates flow-induced endothelial Ca^{2+} influx. Functional evidence also supports a role for TRPV4 in blood pressure regulation in rats. Administration of the TRPV4 selective activator 4α -phorbol 12,13-didecanoate (4α -PDD) leads to dose-dependent decreases in blood pressure (Gao et al., 2009). Here application of specific blockers, demonstrates the hypotensive effect of TRPV4 is mediated, at least in part, by activation of Ca^{2+} -activated K^+ channels (blocked by apamin and charybdotoxin) and CGRP receptors (blocked with CGRP $_{8-37}$) responding to CGRP release from sensory nerves (Gao and Wang, 2010). We found scant evidence for CGRP-IR in the endocardial and myocardial layers of the atrial wall. Where CGRP-IR was occasionally evident on nerve endings in these layers there was coincident TRPV4 labeling and these endings could contribute to volume sensing. Activation of TRPV4 in this location could potentially result in an inhibition in sympathetic nerve activity and a reduction in blood pressure via the well-characterized CNS circuits known to regulate the volume reflex arc (Ledsome and Linden, 1964; Yang and Coote, 2003).

Ca^{2+} -activated K^+ channels

For SK2 most expression was confined within nerves in the epicardium; while wispy SK4-IR was present over limited regions of endocardium, there was no relationship between SK4 and SYN labeling. Immunoreactivity for SK2 was only occasionally found on nerve endings within the myocardium possibly continuing into the endocardium, here it was associated SYN reactivity but the labeling did not strictly coincide. The absence of expression within the putative atrial volume receptor afferents, suggests these channels are unlikely to directly influence afferent sensitivity in this instance. However, SK channels are known to regulate neuronal excitability and levels of intracellular Ca^{2+} (Stocker, 2004). Murine atrial myocytes have been reported to contain SK2 channels where they contribute to cardiac depolarization (Li et al., 2009). By contrast we did not find SK2-IR in the myocardium localized to nerves or myocytes, but there was strong SK2-IR in nerves of the epicardium. We have found SK2-IR both in the terminals of muscle spindle primary endings and in lanceolate endings (F.C. Shenton, unpublished observations) where the SK2 reactivity co-localized with SYN-IR. The SK2 channel was also present in the satellite glial cells with which sensory terminals of the lanceolate endings are very closely associated. However in this present investigation there was no evidence of SK2 channels expressed in putative atrial volume receptors.

A specific SK4 inhibitor has been shown to significantly decrease both basal and stretch-stimulated

491 ANP secretion from an isolated rat atrial preparation
492 (Ogawa et al., 2009). We have demonstrated the
493 presence of SK4-IR in endocardium of the venoatrial
494 junction, where it appeared to be expressed in
495 endothelial cells; thus we postulate this channel could
496 influence the release of ANP from atrial myocytes.

497 We failed to detect immunoreactivity with either anti-
498 SK1 or anti-SK3 antibodies. The SK1 channel is
499 reported to be mostly restricted to the brain (Stocker,
500 2004) although Tuteja et al. (2005) have also found it
501 expressed in isolated rat cardiomyocytes. In our hands
502 the anti-SK3 antibody stains lanceolate endings
503 surrounding hair follicles (Shenton et al., 2010); however
504 this immunoreactivity appeared to be predominantly
505 confined to satellite glial cells surrounding the sensory
506 endings and close to the interface between the endings
507 and the glial cell processes, rather than in the terminals
508 themselves.

509 Compartmentalization

510 The image acquisition and visualization process
511 described in Section 'Image acquisition, visualization
512 and analysis' produced images of a confocal-like quality.
513 The isosurface rendering in particular aids in illustrating
514 the correlation between differently labeled proteins.
515 These views revealed that anti-channel labeling did not
516 precisely coincide with SYN-IR on sensory neurons,
517 suggesting compartmentalization of TRP and SYN
518 proteins within the ending. This was also evident where
519 SK2-SYN co-labeling was seen. SYN is expressed in
520 synaptic-like vesicles in sensory endings (de Camilli
521 et al., 1988; Bewick et al., 2005), while one might
522 expect channel proteins to be preferentially
523 concentrated in the terminal membranes.

524 CONCLUSION

525 This study provides the first evidence as to the possible
526 identity of the mechanosensitive channels that detect
527 blood volume changes and transduce that stimulus into
528 a nervous impulse to initiate the atrial volume reflex arc.
529 Therefore, TRPC1 and TRPV4 proteins should be a
530 focus of future functional investigations to confirm their
531 role in mechanotransduction in atrial volume receptors.

532 Elucidation of the process whereby changes in
533 returning blood volume are detected and signaled to the
534 CNS is necessary to further our understanding of how
535 normal cardiovascular homeostasis malfunctions in
536 heart failure and hypertension. This will require a
537 comprehensive knowledge of the channels and proteins
538 involved. Our study has identified important channel
539 differences between those sensory endings we
540 putatively identify as atrial volume receptors, and the
541 baroreceptor and muscle spindle. These differences
542 may reflect the nature of the stimulus being detected
543 and requires further investigation.

544 Mechanotransduction mechanisms in vertebrates are
545 certain to be diverse and complex, reflecting the broad
546 range of functions they underpin. Other channels and
547 regulatory proteins, in addition to the primary
548 mechanosensitive channels, contribute to the process

(Delmas et al., 2011); nevertheless they may broadly
function in a similar manner, while differing in the detail.
Bewick et al. (2005) demonstrated autogenic modulation
of mechanoreceptor excitability by glutamate release
from SYN positive, synaptic-like vesicles in rat muscle
spindle primary sensory endings, providing an elegant
regulatory model that may pertain to similar
mechanosensitive endings. Our observation of TRPC1
and TRPV4 coincident with abundant SYN-IR in the
venous atrial junction would be compatible with such a
model.

Acknowledgments—This study was funded by an Engineering
and Physical Sciences Research Council Challenging Engineer-
ing Grant (E/F01189X). We thank Dr RW Banks for his help and
advice.

REFERENCES

- Affleck VS, Coote JH, Pyner S (2012) The projection and synaptic
organisation of NTS afferent connections with presympathetic
neurons, GABA and nNOS neurons in the paraventricular nucleus
of the hypothalamus. *Neuroscience* 219:48–61.
- Banks RW, Simon A, Rowe IC, Bewick GS (2009) P/Q type Ca²⁺
channels and K–Ca channels regulate afferent discharge
frequency in spindle mechanosensory terminals. *Soc Neurosci*
172:3.
- Becker D, Blase C, Bereiter-Hahn J, Jendrach M (2005) TRPV4
exhibits a functional role in cell-volume regulation. *J Cell Sci*
118:2435–2440.
- Bewick GS, Reid B, Richardson C, Banks RW (2005) Autogenic
modulation of mechanoreceptor excitability by glutamate release
from synaptic-like vesicles: evidence from the rat muscle spindle
primary sensory ending. *J Physiol* 562:381–394.
- Cheng ZX, Powley TL, Schwaber JS, Doyle FJ (1997) Vagal afferent
innervation of the atria of the rat heart reconstructed with confocal
microscopy. *J Comp Neurol* 381:1–17.
- Coleridge JCG, Hemingway A, Holmes RL, Linden RJ (1957) The
location of atrial receptors in the dog – a physiological and
histological study. *J Physiol* 136. 174.
- Corbett EKA, Sinfield JK, McWilliam PN, Deuchars J, Batten TFC
(2005) Differential expression of vesicular glutamate transporters
by vagal afferent terminals in rat nucleus of the solitary tract:
Projections from the heart preferentially express vesicular
glutamate transporter 1. *Neuroscience* 135(1):133–145.
- de Camilli P, Vitadello M, Canevini MP, Zanoni R, Jahn R, Gorio A
(1988) The synaptic vesicle proteins synapsin 1 and
synaptophysin protein p38 are concentrated both in efferent and
afferent nerve endings of the skeletal muscle. *J Neurosci*
8:1625–1631.
- Delmas P, Hao JZ, Rodat-Despoix L (2011) Molecular mechanisms
of mechanotransduction in mammalian sensory neurons. *Nat Rev*
Neurosci 12:139–153.
- D'Hoedt D, Owsianik G, Prenen J, Cuajungco MP, Grimm C, Heller S,
Voets T, Nilius B (2008) Stimulus-specific modulation of the cation
channel TRPV4 by PACSIN 3. *J Biol Chem* 283:6272–6280.
- Drummond HA, Price MP, Welsh MJ, Abboud FM (1998) A molecular
component of the arterial baroreceptor mechanotransducer.
Neuron 21:1435–1441.
- Feetham C, Barrett-Jolley R (2012) Volume control in the PVN: a role
for TRPV4. *Biophys J* 102. 546A–546A.
- Fu Y, Subramanya A, Rozansky D, Cohen DM (2006) WNK kinases
influence TRPV4 channel function and localization. *Am J Physiol*
290:F1305–F1314.
- Gao F, Wang DH (2010) Hypotension induced by activation of the
transient receptor potential vanilloid 4 channels: role of Ca²⁺-

- 612 activated K⁺ channels and sensory nerves. *J Hypertens*
613 28:102–110.
- 614 Gao F, Sui DX, Garavito M, Worden RM, Wang DH (2009) Salt intake
615 augments hypotensive effects of transient receptor potential
616 vanilloid 4 functional significance and implication. *Hypertension*
617 53:228–235.
- 618 Girard BM, Merrill L, Malley S, Vizzard MA (2013) Increased TRPV4
619 expression in urinary bladder and lumbosacral dorsal root ganglia
620 in mice with chronic overexpression of NGF in urothelium. *J Mol*
621 *Neurosci* 51:602–614.
- 622 Glazebrook PA, Schilling WP, Kunze DL (2005) TRPC channels as
623 signal transducers. *Pflugers Arch* 451:125–130.
- 624 Hainsworth R (1991) Reflexes from the heart. *Physiol Rev*
625 71:617–658.
- 626 Holmes RL (1957) Structures in the atrial endocardium of the dog
627 which stain with methylene blue, and the effects of unilateral
628 vagotomy. *J Anat* 91:259–266.
- 629 Huai J, Zhang Y, Liu QM, Ge HY, Arendt-Nielsen L, Jiang H, Yue SW
630 (2012) Interaction of transient receptor potential vanilloid 4 with
631 annexin A2 and tubulin beta 5. *Neurosci Lett* 512:22–27.
- 632 Hunt CC, Wilkinson RS, Fukami Y (1978) Ionic basis of receptor
633 potential in primary endings of mammalian muscle-spindles. *J*
634 *Gen Physiol* 71:683–698.
- 635 Inoue R, Jian Z, Kawarabayashi Y (2009) Mechanosensitive TRP
636 channels in cardiovascular pathophysiology. *Pharmacol Ther*
637 123:371–385.
- 638 Jung S, Muhle A, Schaefer M, Strotmann R, Schultz G, Plant TD
639 (2003) Lanthanides potentiate TRPC5 currents by an action at
640 extracellular sites close to the pore mouth. *J Biol Chem*
641 278:3562–3571.
- 642 Kappagoda CT, Linden RJ, Mary D (1976) Atrial receptors in cat. *J*
643 *Physiol* 262:431–446.
- 644 Kappagodda CT, Linden RJ, Snow HM (1973) Effect of stimulating
645 right atrial receptors on urine flow in dog. *J Physiol* 235:493–502.
- 646 Katz B (1966) *Nerve, muscle, and synapse*. McGraw-Hill Book Co.
- 647 Ledsome JR, Linden RJ (1964) Reflex increase in heart rate from
648 distension of pulmonary–vein–atrial junctions. *J Physiol* 170: 456.
- 649 Lee CH, Sun SH, Lin SH, Chen CC (2011) Role of the acid-sensing
650 ion channel 3 in blood volume control. *Circ J* 75:874–883.
- 651 Li N, Timofeyev V, Tuteja D, Xu DY, Lu L, Zhang Q, Zhang Z,
652 Singapur A, Albert TR, Rajagopal AV, Bond CT, Periasamy M,
653 Adelman J, Chiamvimonvat N (2009) Ablation of a Ca²⁺-activated
654 K⁺ channel (SK2 channel) results in action potential prolongation
655 in atrial myocytes and atrial fibrillation. *J Physiol* 587:1087–1100.
- 656 Lu YJ, Ma XY, Sabharwal R, Snitsarev V, Morgan D, Rahmouni K,
657 Drummond HA, Whiteis CA, Costa V, Price M, Benson C, Welsh
658 MJ, Chappleau MW, Abboud FM (2009) The ion channel ASIC2 is
659 required for baroreceptor and autonomic control of the circulation.
660 *Neuron* 64:885–897.
- 661 Ma X, Qiu S, Luo JH, Ma Y, Ngai CY, Shen B, Wong CO, Huang Y,
662 Yao XQ (2010) Functional role of vanilloid transient receptor
663 potential 4-canonical transient receptor potential 1 complex in
664 flow-induced Ca²⁺ influx. *Arterioscler Thromb Vasc Biol*
665 30:851–858.
- 666 Maeda T, Ochi K, Nakakura-Ohshima K, Youn SH, Wakisaka S
667 (1999) The Ruffini ending as the primary mechanoreceptor in the
668 periodontal ligament: Its morphology, cytochemical features,
669 regeneration, and development. *Crit Rev Oral Biol Med*
670 10:307–327.
- 671 Meacci E, Bini F, Sassoli C, Martinesi M, Squecco R, Chellini F,
672 Zecchi-Orlandini S, Francini F, Formigli L (2010) Functional
673 interaction between TRPC1 channel and connexin-43 protein: a
674 novel pathway underlying S1P action on skeletal myogenesis.
675 *Cell Mol Life Sci* 67:4269–4285.
- 676 Ogawa T, Forero M, Burgon PG, de Bold MLK, Georgalis T, de Bold
677 AJ (2009) Role of potassium channels in stretch-promoted atrial
678 natriuretic factor secretion. *J Am Soc Hypertens* 3:9–18.
- 679 Oh-hashii Y, Shindo T, Kurihara Y, Imai T, Wang YH, Morita H, Imai
680 Y, Kayaba Y, Nishimatsu H, Suematsu Y, Hirata Y, Yazaki Y,
681 Nagai R, Kuwaki T, Kurihara H (2001) Elevated sympathetic
682 nervous activity in mice deficient in alpha CGRP. *Circ Res*
683 89:983–990.
- 684 Paintal AS (1953) A study of right and left atrial receptors. *J Physiol*
685 120:596–610.
- 686 Ramsey IS, Delling M, Clapham DE (2006) An introduction to TRP
687 channels. *Annu Rev Physiol* 68:619–647.
- 688 Shenton FC, Banks RW, Bewick GS (2010) In lanceolate endings of
689 rat hair follicles the small conductance Ca²⁺-activated K⁺
690 channel SK3 is found mainly in glial cells. *Proc Physiol Soc* 21.
691 C15, PC15.
- 692 Simon A, Shenton F, Hunter I, Banks RW, Bewick GS (2010)
693 Amiloride-sensitive channels are a major contributor to
694 mechanotransduction in mammalian muscle spindles. *J Physiol*
695 588:171–185.
- 696 Skofitsch G, Jacobowitz DM (1985) Calcitonin gene-related peptide -
697 detailed immunohistochemical distribution in the central nervous-
698 system. *Peptides* 6:721–745.
- 699 Spyer KM (1994) Annual-review prize lecture – central nervous
700 mechanisms contributing to cardiovascular control. *J Physiol*
701 474:1–19.
- 702 Stocker M (2004) Ca²⁺-activated K⁺ channels: molecular
703 determinants and function of the SK family. *Nat Rev Neurosci*
704 5:758–770.
- 705 Sullivan MJ, Sharma RV, Wachtel RE, Chappleau MW, Waite LJ,
706 Bhalla RC, Abboud FM (1997) Non-voltage-gated Ca²⁺ influx
707 through mechanosensitive ion channels in aortic baroreceptor
708 neurons. *Circ Res* 80:861–867.
- 709 Suzuki M, Hirao A, Mizuno A (2005) Microtubule-associated protein 7
710 increases the membrane expression of transient receptor
711 potential vanilloid 4 (TRPV4). *J Biol Chem* 280: 25948–25948.
- 712 Thoren P, Noresson E, Ricksten SE (1979) Cardiac receptors with
713 non-medullated vagal afferents in the rat. *Acta Physiol Scand*
714 105:295–303.
- 715 Tranumjensen J (1975) Ultrastructure of sensory end-organs
716 (baroreceptors) in atrial endocardium of young mini-pigs. *J Anat*
717 119:255–275.
- 718 Tuteja D, Xu DY, Timofeyev V, Lu L, Sharma D, Zhang Z, Xu YF, Nie
719 LP, Vazquez AE, Young JN, Glatzer KA, Chiamvimonvat N (2005)
720 Differential expression of small-conductance Ca²⁺-activated K⁺
721 channels SK1, SK2, and SK3 in mouse atrial and ventricular
722 myocytes. *Am J Physiol* 289:H2714–H2723.
- 723 Watanabe H, Murakami M, Ohba T, Takahashi Y, Ito H (2008) TRP
724 channel and cardiovascular disease. *Pharmacol Ther*
725 118:337–351.
- 726 Woollard HH (1926) The innervation of the heart. *J Anat* 60:
727 345–373.
- 728 Yang Z, Coote JH (2003) Role of GABA and NO in the paraventricular
729 nucleus-mediated reflex inhibition of renal sympathetic nerve
730 activity following stimulation of right atrial receptors in the rat. *Exp*
731 *Physiol* 88:335–342.

(Accepted 27 February 2014)
(Available online xxxx)